Imaging Agents

DOI: 10.1002/ange.200901005

Symmetry-Guided Design and Fluorous Synthesis of a Stable and Rapidly Excreted Imaging Tracer for ^{19}F MRI**

*Zhong-Xing Jiang, Xin Liu, Eun-Kee Jeong, and Yihua Bruce Yu**

^{1}H and ^{19}F are the most sensitive nuclei for nuclear magnetic resonance imaging (MRI), with the ^{1}H signal suited for collecting information about the body[1,2] and the ^{19}F signal suited for collecting information about drugs in the body.[3,4] Although ^{19}F MRI[5] is only four years younger than ^{1}H MRI,[6] it is not in clinical use. The progress of ^{19}F MRI has been stalled by the lack of suitable imaging agents. Current ^{19}F imaging agents are perfluorocarbon (PFC) emulsions[7–13] and suffer severe shortcomings, including heterogeneity, instability, split ^{19}F signals, complex formulation procedure and, most importantly, excessive retention of the agent within organs for months or longer.[8,14] We developed a bispherical fluorocarbon molecule, denoted as ^{19}FIT to stand for ^{19}F imaging tracer, which overcame all the major deficiencies of PFC-based imaging agents. ^{19}FIT, designed using the principle of modular spherical symmetry, is water soluble and emits a single ^{19}F signal from 27 fluorine atoms. The in vivo residence half-life of ^{19}FIT measured in mice is about 0.5 day, and no evidence of organ retention or in vivo degradation was found. Our result shows that modular symmetry is a useful strategy for designing molecules with multiple functionalities. With suitable imaging agents like ^{19}FIT, ^{19}F MRI has the potential to play an important role in drug therapy, analogous to the role played by ^{1}H MRI in disease diagnosis.

MRI has made significant contribution to medical diagnosis.[15] The value of MRI comes from its ability to collect in vivo information noninvasively without ionizing radiation.[16] ^{1}H and ^{19}F are the most and second most sensitive stable nuclei for MRI, respectively. Because of the ubiquitous presence of the ^{1}H signal and the complete absence of the ^{19}F signal in the human body, ^{1}H and ^{19}F MRI complement each other in their information content. ^{1}H MRI is suited for collecting information about the body (anatomy, physiology, and biochemistry) and is therefore a valuable tool for disease diagnosis. ^{19}F MRI, on the other hand, is a tracer-type technology and is suited for collecting information about drugs in the body (where, how much, and in what form), and therefore has the potential to become a valuable tool for image-guided drug therapy.

Direct monitoring of drugs by ^{19}F MRI requires the drug to be labeled by appropriate ^{19}F imaging agents. For more than three decades, PFC emulsions have been used as ^{19}F imaging agents.[5,7–13] However, PFC emulsions suffer severe drawbacks as imaging agents. First and foremost, PFCs are very lipophilic and accumulate excessively in internal organs (liver, spleen, lung) for months or longer.[8,14] Second, emulsion droplets are inherently heterogeneous, unstable, and likely to disintegrate inside the body. In fact, the in vivo integrity of PFC droplets is difficult, if not impossible, to verify. Third, linear PFCs emit multiple ^{19}F signals because of the lack of symmetry. Signal splitting lowers signal intensity and can cause image artifacts. Macrocyclic PFCs (e.g., perfluoro[15]crown-5 ether (PF15C5)) will also emit multiple ^{19}F signals if covalently modified because their cyclic symmetry will then be broken. Finally, the formulation of PFC emulsions is quite complex, requiring multiple surfactants and microfluidic devices.[11–13] Complex formulation brings a range of difficulties for industrial production and regulatory approval. Indeed, there is currently only one injectable emulsion, Diprivan, on the U.S. market.[17]

All the aforementioned shortcomings of PFC-based imaging agents can be avoided if a stable, hydrophilic molecule which emits a single ^{19}F signal from multiple fluorine atoms can be developed. To achieve this goal, we employed a molecular design principle called modular spherical symmetry. A molecule with modular spherical symmetry comprises independent spherical cones joined by covalent bonds in the cone part. The fluorocarbon molecule ^{19}FIT contains an F-spherical cone and an H-spherical cone (Figure 1). Spherical symmetry in the F-spherical cone ensures a single ^{19}F signal from multiple fluorine atoms. Spherical symmetry in the H-spherical cone allows efficient incorporation of multiple hydrophilic groups. The advantage of spherical cones over macrocycles is that a spherical cone can be modified at the cone without breaking the symmetry of the sphere, whereas a macrocycle will lose its cyclic symmetry upon modification. ^{19}FIT comprises three building blocks, **I**,

[*] Prof. Y. B. Yu
Department of Pharmaceutical Sciences
University of Maryland, Baltimore MD (USA)
Fax: (+1) 410-706-5017
E-mail: byu@rx.umaryland.edu
Homepage: http://www.bioe.umd.edu/facstaff/yu.html
Dr. Z.-X. Jiang, Prof. Y. B. Yu
Fischell Department of Bioengineering
University of Maryland, College Park (USA)
X. Liu
Department of Physics, University of Utah
Salt Lake City (USA)
Prof. E.-K. Jeong
Department of Radiology, University of Utah
Salt Lake City (USA)

[**] This work was supported by NIH grants (EY015181 & EB004416), the Maryland Nano-Biotechnology Fund and the University of Utah seed incentive grant. We thank Dr. Yong-En Sun for assisting with animal handling. MRI = magnetic resonance imaging.

Supporting information for this article is available on the WWW under http://dx.doi.org/10.1002/anie.200901005.

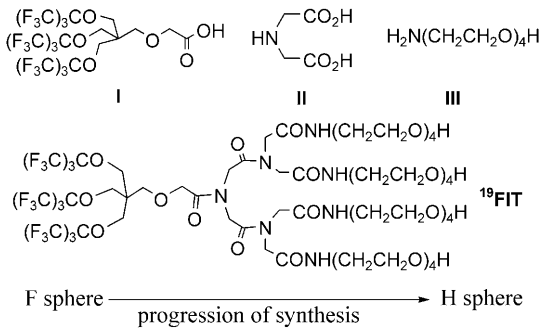

Figure 1. Chemical structures of ^{19}FIT and its three building blocks (**I**, **II**, and **III**). ^{19}FIT is designed to be a bispherical cone. The F sphere contains 27 fluorine atoms for ^{19}F signal generation. The H sphere, currently made of 4 OH groups, can be derivatized to COOH, NH_2, and SH for future drug conjugation.[23]

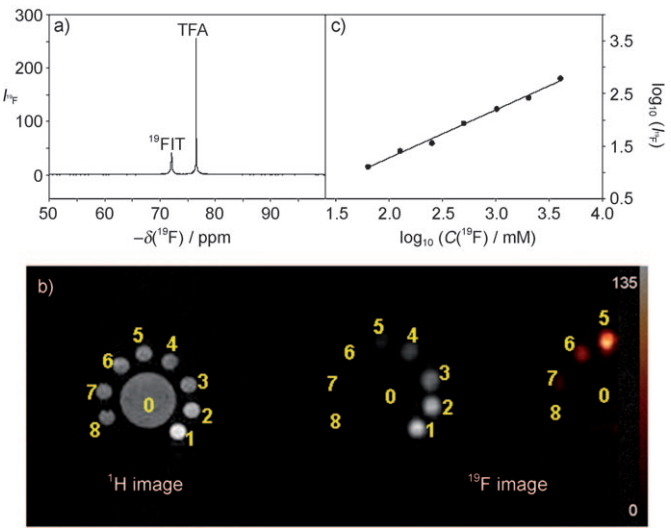

Figure 2. a) ^{19}F NMR spectrum of ^{19}FIT in PBS. TFA is the internal ^{19}F standard. b) ^{1}H and ^{19}F MRI images of phantoms (1–8) filled with ^{19}FIT in PBS. ^{19}F concentrations in the phantoms are: 4050 mM, 2025 mM, 1012 mM, 506 mM, 253 mM, 126 mM, 63 mM, and 32 mM for phantoms 1–8, respectively. Phantom 0 contains water. ^{19}F images of the phantoms were given in two color schemes: white/black (for high-concentration phantoms) and red/black (for low-concentration phantoms). c) Plot of $\log_{10}(I_{^{19}F})$ versus $\log_{10}(C(^{19}F))$. C = concentration.

II, and **III**, with **I** being the ^{19}F signal emitter, and **II** and **III** serving to enhance the aqueous solubility of the tracer (Figure 1). ^{19}FIT was synthesized in a sequential manner which involved repetitive deprotection/condensation cycles (Scheme 1), analogous to solid-phase peptide synthesis. The synthesis proceeded from the F sphere to the H sphere so that all synthesis intermediates (**2**, **I**, and **3**–**7**) contained nine CF_3 groups and could thereby be purified by using the unique separation power of fluorous chemistry.[18,19] The final product, ^{19}FIT, was purified using a combination of fluorous silica gel chromatography and preparative HPLC methods (see Figure S1 in the Supporting Information).

^{19}FIT is soluble in phosphate-buffered saline (PBS, Figure S2) and emits a single ^{19}F signal from 27 fluorine atoms (Figure 2a). ^{19}F NMR study shows that ^{19}FIT forms micelles in PBS with a critical micelle concentration of approximately 7 mM (Figure S3). Phantom experiments show that the ^{19}F signal intensity is indeed proportional to ^{19}F concentration (Figure 2b and c). The ^{19}F longitudinal relaxation time, T_1, of ^{19}FIT is much shorter than that of PF15C5 when measured under the same experimental conditions (163 ms versus 1069 ms). Even with 30 mol% of relaxation-enhancing Gd^{3+}, the ^{19}F T_1 value of PF15C5 reported in the literature[11] is still significantly longer than that of ^{19}FIT. The smaller T_1 value is yet another advantage of using ^{19}FIT over PFCs as it reduces data collection time and thereby increases signal intensity.[20,21]

A 150 mM ^{19}FIT PBS solution was administered to 16-week-old BALB/c male mice at two dose levels: either 400 μL per mouse (ca. 60 mmol kg^{-1} ^{19}F), or 200 μL per mouse (ca. 30 mmol kg^{-1} ^{19}F). At both dose levels, the ^{19}F signal decreased rapidly and became invisible in all organs, except the bladder, after 1–2 hours (Figure 3 and Figure S4). The ^{19}F signal intensity also decreased rapidly in whole-body ^{19}F spectra and in urine samples collected from mice injected with ^{19}FIT (Figure 4a and Figure S5). On the basis of the ^{19}F signal intensity decays of both the whole-body and urine samples, the in vivo residence half-life, $t_{1/2}$, of ^{19}FIT is estimated to be approximately 0.5 day. In comparison, the in vivo residence half-lives of perfluorocarbons, also determined by ^{19}F MRI, are months or longer.[8]

Whole-body ^{19}F spectra in different mice showed only one ^{19}F peak at all time

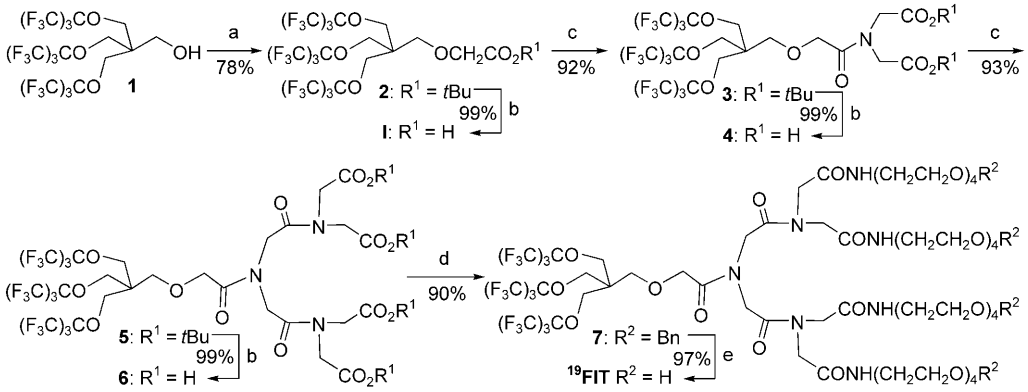

Scheme 1. The synthesis of ^{19}FIT. Reaction conditions: a) KH, $BrCH_2CO_2tBu$, THF, RT, 12 h; b) TFA, anisole, CH_2Cl_2, RT, 2 h; c) DIC, HOBt, DMF/THF (1:1), $HN(CH_2CO_2tBu)_2$ (= **II**-(tBu)$_2$), RT, 12 h; d) DIC, HOBt, DMF/THF (1:1), $H_2N(CH_2CH_2O)_4Bn$ (= **III**-Bn), RT, 18 h; e) H_2, Pd/C, MeOH, RT, 12 h. TFA = trifluoroacetic acid, DIC = 1,3-diisopropylcarbodiimide, HOBT = 1-hydroxytriazole, DMF = *N*,*N*′-dimethylformamide, THF = tetrahydrofuran Bn = benzyl.

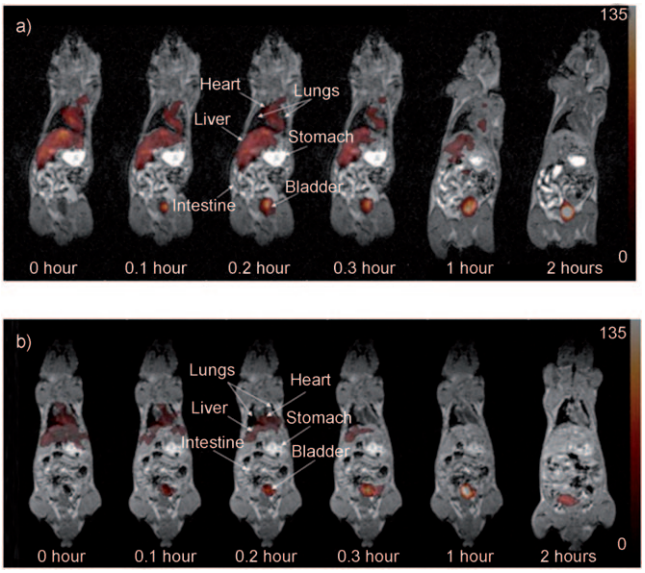

Figure 3. Superimposed ^{1}H (white) and ^{19}F (red) images (coronal view) of mouse 1 (a) and 3 (b). Mice 1 and 3 were injected with 400 μL (60 mmol kg^{-1} ^{19}F) and 200 μL (30 mmol kg^{-1} ^{19}F) of 150 mM ^{19}FIT PBS solution, respectively. For images beyond 2 h, see Figure S4.

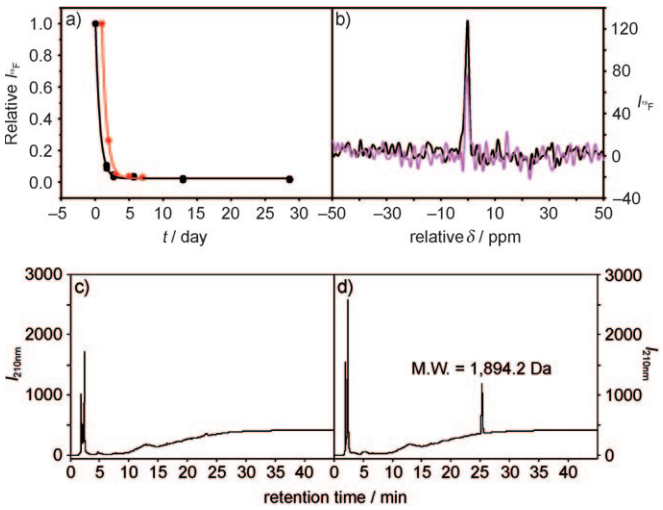

Figure 4. a) ^{19}F signal intensity decay with time. Black symbols: whole-body ^{19}F signals from mice 1 and 2 collected using a 3.0 T clinical magnetic resonance scanner. Red symbols: mouse 6 urine ^{19}F signal collected using an 11.7 T NMR spectrometer. For each series, the first data point is normalized to one. The curves are fitting data to single-component exponential decay. b) In vivo ^{19}F spectra for mouse 1 at 8220 min (black) and mouse 3 at 8880 min (pink). The maximum position of each signal is manually set to 0 ppm. The ratio of the two signal intensities is 2.08, about the same as the dose ratio between these two mice, which is 2.0. For more in vivo ^{19}F spectra, see Figure S6. c, d) HPLC chromatograms of urine collected from mouse 6 one day before (c) and one day after (d) receiving ^{19}FIT.

points (Figure 4b and Figure S6). There is also only one ^{19}F peak in all urine samples, having the same chemical shift as ^{19}FIT (Figure S7). A comparison of the HPLC profiles of the urine samples collected before and after the injection of ^{19}FIT showed only one peak, which was attributable to fluorinated compounds (Figures 4c and d). The mass of this peak is 1894.2 Da, the same as intact ^{19}FIT. All these results are consistent with no in vivo degradation of ^{19}FIT. Mice injected with ^{19}FIT were observed for up to 45 days and showed no sign of acute toxicity or weight loss.

In summary, ^{19}FIT overcomes major deficiencies of PFC-based ^{19}F imaging agents, including heterogeneity, instability, split ^{19}F signals, large ^{19}F T_1 values, complex formulation, and, most importantly, excessive retention of the tracer within the organ. With suitable imaging agents, ^{19}F MRI has the potential to play an important role in drug therapy, analogous to the role played by ^{1} MRI in disease diagnosis. From a chemistry standpoint, bispherical symmetry is a step forward from the unispherical symmetry employed in conventional dendrimer design.[22] In fact, modular symmetry is a general molecular design principle that can be extended to trispherical symmetry and beyond.

The application of ^{19}FIT to drug or cell monitoring using ^{19}F MRI still faces stiff challenges. One issue is sensitivity. The approach of using symmetry to generate a single ^{19}F signal from multiple fluorine atoms can only go so far, on the order of 100 fluorine atoms. Other approaches, such as using paramagnetic ions to reduce the T_1 and T_2 values of ^{19}F,[11,20,21] are needed. Another issue is a dilemma common to all labeling tags; if the labeling is noncovalent, then the tag might dissociate from the drugs or cells, and signals from free and bound tags can hardly be distinguished. However, if the labeling is covalent, then the tag might alter the bioactivity of drugs or cells. One possible solution to this dilemma is to use the prodrug approach, that is, making ^{19}FIT–drug into a prodrug which replaces the free drug as the therapeutic agent. The pharmacologically inactive ^{19}FIT–drug will be converted into the active free drug at the pathological site (e.g., tumor). The pharmacokinetics of ^{19}FIT can be monitored with ^{19}F MRI right up to the point where ^{19}FIT–drug is converted into the free drug at the disease site, with the ^{19}FIT–drug→ ^{19}FIT + drug conversion process monitored by ^{19}F MRS. We are currently pursing these approaches.

Experimental Section

Synthesis of ^{19}FIT:

$$\mathbf{1} \xrightarrow{a} \mathbf{2} \xrightarrow{b} \mathbf{I} \xrightarrow{c} \mathbf{3} \xrightarrow{b} \mathbf{4} \xrightarrow{c} \mathbf{5} \xrightarrow{b} \mathbf{6} \xrightarrow{d} \mathbf{7} \xrightarrow{e} {}^{19}\text{FIT} \quad (1)$$

tert-Butyl monoester **2** (procedure a): A suspension of potassium hydride (30%, 3.2 g, 24.0 mmol) was added slowly to a stirred solution of alcohol **1**[23] (15.8 g, 20.0 mmol) in tetrahydrofuran (200 mL) at 0 °C. After 10 min, *tert*-butyl bromoacetate (5.9 mL, 7.8 g, 40.0 mmol) was added to the suspension in one portion at RT and the resulting mixture was stirred at RT overnight. After the reaction mixture had been quenched with water (20 mL), the mixture was transferred into a separatory funnel and the lower phase was collected as a clear oil. The low-boiling-point impurities were then removed under vacuum and the monoester **2** was obtained as a clear oil (14.1 g, 78% yield). ^{1}H NMR (400 MHz, $CDCl_3$): $\delta = 4.14$ (s, 6H), 3.91 (s, 2H), 3.57 (s, 2H), 1.46 ppm (s, 9H); ^{19}F NMR (376 MHz, $CDCl_3$): $\delta = -73.51$ ppm (s); ^{13}C NMR (100.7 MHz, $CDCl_3$): $\delta =$ 168.5, 120.2 (q, $J = 293.4$ Hz), 81.8, 79.1–80.0 (m), 69.2, 67.2, 66.2, 46.1, 27.9 ppm; MS (ESI) m/z 905 ($[M+1]^+$); HRMS (MALDI-TOF) calcd for $C_{23}H_{20}F_{27}O_6$ 905.0829, found 905.0823.

Monoacid **I** (procedure b): Trifluoroacetic acid (30 mL) was added to a stirred solution of *tert*-butyl ester **2** (13.6 g, 15.0 mmol) and anisole (3.0 mL) in dichloromethane (100 mL) at RT, and the resulting solution was stirred at RT for 2 h. After the reaction mixture was evaporated to dryness under vacuum, the residue was dissolved in methanol/toluene (50 mL:30 mL) and evaporated to dryness under vacuum to give the monoacid **I** as a reddish oil (12.6 g, 99% yield) which was used in the next step without further purification. ^{1}H NMR (400 MHz, [D$_6$]acetone): $\delta = 4.29$ (s, 6H), 4.14 (s, 2H), 3.73 ppm (s, 2H); ^{19}F NMR (376 MHz, [D$_6$]acetone): $\delta = -71.24$ ppm (s); ^{13}C NMR (100.7 MHz, [D$_6$]acetone): $\delta = 170.9$, 121.2 (q, $J = 292.5$ Hz), 80.1–81.0 (m), 68.6, 67.5, 67.1, 47.1 ppm; MS (ESI) m/z 848 [M^+]; HRMS (MALDI-TOF) calcd for $C_{19}H_{12}F_{27}O_6$ 849.0203, found 849.0197.

Monoamide **3** (procedure c): 1,3-Diisopropylcarbodiimide (6.6 mL, 5.4 g, 42.5 mmol) was added to a stirred solution of 1-hydroxytriazole (5.7 g, 42.5 mmol) and acid **I** (12.0 g, 14.2 mmol) in dry *N*,*N*-dimethylformamide (200 mL) at RT. After stirring for 15 min, di-*tert*-butyl iminodiacetate (**II**-(*t*Bu)$_2$) (10.4 g, 42.5 mmol) was added and the resulting mixture was stirred at RT for 12 h. Water (20 mL) was added to the reaction mixture and the resulting mixture was concentrated and purified by solid-phase extraction on Fluoroflash silica gel, with H_2O and CH_3OH (1:4) as eluents, to give the monoamide **3** as a clear oil (14.1 g, 92% yield) which was used in the next step without further purification. ^{1}H NMR (400 MHz, $CDCl_3$): $\delta = 4.12$ (s, 6H), 4.10 (s, 2H), 4.02 (s, 2H), 3.92 (s, 2H), 3.59 (s, 2H), 1.44 (s, 9H), 1.42 ppm (s, 9H); ^{19}F NMR (376 MHz, $CDCl_3$): $\delta = -73.29$ ppm (s); ^{13}C NMR (100.7 MHz, $CDCl_3$): $\delta = 168.7$, 167.9, 167.7, 120.1 (q, $J = 293.4$ Hz), 82.8, 82.0, 78.7–79.8 (m), 69.5, 67.7, 66.5, 49.9, 48.6, 46.0, 27.8, 27.76 ppm; MS (MALDI-TOF) m/z 1098 ([M+Na]$^+$); HRMS (MALDI-TOF) calcd for $C_{31}H_{32}F_{27}NNaO_9$ 1098.1544, found 1098.1538.

^{19}FIT (procedure e): A mixture of heptaamide **7** (5.5 g, 2.5 mmol) and palladium on carbon (10%, 2.5 g) in methanol (200 mL) was stirred under a hydrogen atmosphere (50 bar) over 12 h at RT. After the mixture had been filtered through a pad of celite, it was concentrated and purified by HPLC on a preparative Fluoroflash column with H_2O and CH_3OH as eluents to give the pure ^{19}FIT as a wax (4.5 g, 97% yield). The purity of ^{19}FIT was verified using analytical HPLC (Figure S1). ^{1}H NMR (400 MHz, CD_3OD) δ 4.26 (s, 2H), 4.25 (s, 8H), 4.22 (s, 2H), 4.18 (s, 2H), 4.15 (s, 2H), 4.05 (s, 2H), 4.04 (s, 2H), 3.59–3.67 (m, 42H), 3.53–3.58 (m, 16H), 3.44 (t, $J =$ 4.2 Hz, 4H), 3.38 (t, $J = 5.6$ Hz, 4H); ^{19}F NMR (376 MHz, CD_3OD) $\delta = -71.05$ (s); ^{13}C NMR (100.7 MHz, CD_3OD): $\delta = 172.3$, 171.9, 171.3, 171.27, 171.1, 170.8, 170.5, 121.6 (q, $J = 292.5$ Hz), 80.3–81.5 (m), 73.7, 71.6, 71.4, 71.2, 71.18, 71.1, 70.4, 70.3, 69.5, 68.7, 68.3, 62.2, 53.2, 53.0, 52.5, 49.7, 47.2, 40.5, 40.4; MS (MALDI-TOF) m/z 1916 ([M + Na]$^+$); HRMS (MALDI-TOF) calcd for $C_{63}H_{94}F_{27}N_7NaO_{27}$ 1916.5664, found 1916.5642.

For additional synthetic procedures, as well as the MRI and metabolic studies, see the Supporting Information.

Received: February 20, 2009
Published online: May 27, 2009

Keywords: ^{19}F MRI spectroscopy · dendrimers · imaging agents · modular symmetry · fluorine

[1] P. C. Lauterbur, *Angew. Chem.* **2005**, *117*, 1026 – 1034; *Angew. Chem. Int. Ed.* **2005**, *44*, 1004 – 1011.
[2] P. Mansfield, *Angew. Chem.* **2004**, *116*, 5572 – 5580; *Angew. Chem. Int. Ed.* **2004**, *43*, 5456 – 5464.
[3] J.-X. Yu, V. D. Kodibagkar, W. Cui, R. P. Mason, *Curr. Med. Chem.* **2005**, *12*, 819 – 848.
[4] W. Wolf, C. A. Presant, V. Waluch, *Adv. Drug Delivery Rev.* **2000**, *41*, 55 – 74.
[5] G. N. Holland, P. A. Bottomley, W. S. Hinshaw, *J. Magn. Reson.* **1977**, *28*, 133 – 136.
[6] P. C. Lauterbur, *Nature* **1973**, *242*, 190 – 191.
[7] R. P. Mason, P. P. Antich, E. E. Babcock, J. L. Gerberich, R. L. Nunnally, *Magn. Reson. Imaging* **1989**, *7*, 475 – 485.
[8] K. L. Meyer, M. J. Carvlin, B. Mukherji, H. A. Sloviter, P. M. Joseph, *Invest. Radiol.* **1992**, *27*, 620 – 627.
[9] A. M. Morawski, P. M. Winter, X. Yu, R. W. Fuhrhop, M. J. Scott, F. Hockett, J. D. Robertson, P. J. Gaffney, G. M. Lanza, S. A. Wickline, *Magn. Reson. Med.* **2004**, *52*, 1255 – 1262.
[10] E. T. Ahrens, R. Flores, H. Xu, P. A. Morel, *Nat. Biotechnol.* **2005**, *23*, 983 – 987.
[11] A. M. Neubauer, J. Myerson, S. D. Caruthers, F. D. Hocket, P. M. Winter, J. Chen, P. J. Gaffney, J. D. Robertson, G. M. Lanza, S. A. Wickline, *Magn. Reson. Med.* **2008**, *60*, 1066 – 1072.
[12] J. M. Janjic, M. Srinivas, D. K. K. Kadayakkara, E. T. Ahrens, *J. Am. Chem. Soc.* **2008**, *130*, 2832 – 2841.
[13] A. Kimura, M. Narazaki, Y. Kanazawa, H. Fujiwara, *Magn. Reson. Imaging* **2004**, *22*, 855 – 860.
[14] Y. Nosé, *Artif. Organs* **2004**, *28*, 807 – 812.
[15] J. Gore, *N. Engl. J. Med.* **2003**, *349*, 2290 – 2292.
[16] J. K. Willmann, N. van Bruggen, L. M. Dinkelborg, S. S. Gambhir, *Nat. Rev. Drug Discovery* **2008**, *7*, 591 – 607.
[17] R. G. Strickley, *Pharm. Res.* **2004**, *21*, 201 – 230.
[18] I. T. Horváth, J. Rábai, *Science* **1994**, *266*, 72 – 75.
[19] D. P. Curran, *Synlett* **2001**, 1488 – 1496.
[20] A. V. Ratner, S. Quay, H. H. Muller, B. B. Simpson, R. Hurd, S. W. Young, *Invest. Radiol.* **1989**, *24*, 224 – 227.
[21] H. Lee, R. R. Price, G. E. Holburn, C. L. Partain, M. D. Adams, W. P. Catheris, *Magn. Reson. Imaging* **1994**, *4*, 609 – 613.
[22] D. A. Tomalia, L. A. Reyna, S. Svenson, *Biochem. Soc. Trans.* **2007**, *35*, 61 – 67.
[23] Z.-X. Jiang, Y. B. Yu, *Tetrahedron* **2007**, *63*, 3982 – 3988.
[24] Z.-X. Jiang, Y. B. Yu, *Synthesis* **2008**, 215 – 220.

